

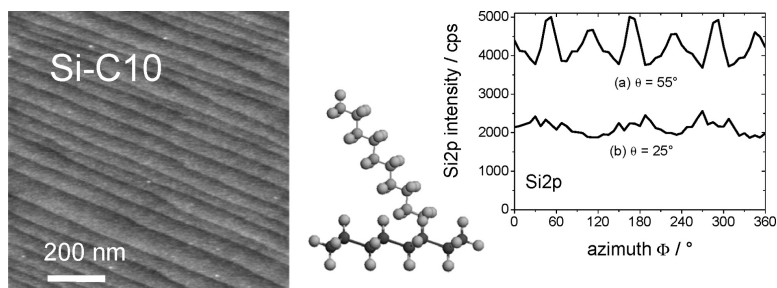
Article

Truly Quantitative XPS Characterization of Organic Monolayers on Silicon: Study of Alkyl and Alkoxy Monolayers on H-Si(111)

Xavier Wallart, Catherine Henry de Villeneuve, and Philippe Allongue

J. Am. Chem. Soc., **2005**, 127 (21), 7871-7878 • DOI: 10.1021/ja0430797 • Publication Date (Web): 06 May 2005

Downloaded from <http://pubs.acs.org> on March 25, 2009



More About This Article

Additional resources and features associated with this article are available within the HTML version:

- Supporting Information
- Links to the 20 articles that cite this article, as of the time of this article download
- Access to high resolution figures
- Links to articles and content related to this article
- Copyright permission to reproduce figures and/or text from this article

[View the Full Text HTML](#)



ACS Publications
 High quality. High impact.

Truly Quantitative XPS Characterization of Organic Monolayers on Silicon: Study of Alkyl and Alkoxy Monolayers on H–Si(111)

Xavier Wallart,^{*,†} Catherine Henry de Villeneuve,[‡] and Philippe Allongue^{*,‡}

Contribution from the Institut d'Electronique, de Microélectronique et de Nanotechnologie, CNRS-UMR 8520, Avenue Poincaré, B.P. 69, 59652 Villeneuve d'Ascq Cedex, France, and Laboratoire de Physique de la Matière Condensée, CNRS-UMR 7643, Ecole Polytechnique, 91128 Palaiseau, France

Received November 17, 2004; E-mail: Xavier.Wallart@iemn.univ-lille1.fr; Philippe.Allongue@Polytechnique.fr

Abstract: The quantitative characterization of the chemical composition (bonding at grafted and ungrafted sites, surface coverage) is a key issue for the application of silicon–organic monolayer hybrid interfaces. The primary purpose of this article is to demonstrate that X-ray photoelectron spectroscopy (XPS) requires to be truly quantitative to deal with two main questions. The first one is accounting for X-ray photodiffraction (XPD), a well-known phenomenon that is responsible for azimuthal variations of the XPS signal intensity. A simple procedure is proposed to account for XPD in angle-resolved measurements. The second critical point concerns the choice of photoelectron attenuation lengths (AL). This article demonstrates that *n*-alkanethiol self-assembled monolayers on Au(111) can be used as a *reference* system to derive the *effective* monolayer thickness on silicon substrates and that one may use the empirical relationship established by Laibinis and co-workers to calculate the relevant ALs (Laibinis, P. E.; Bain, C. D.; Whitesides, G. M. *J. Phys. Chem.* **1991**, *95*, 7017). A self-consistent approach is presented to justify the above assertions and to give a complete compositional description of alkyl and alkoxy monolayers directly grafted on atomically flat H–Si(111) surfaces. Direct evidences are provided that a Si–C and a Si–O–C linkage is formed, respectively, after reaction with decene and decanol and that the ungrafted sites remain saturated with H atoms. Moreover, the quantitative spectra analysis of satellite peaks at fixed polar angle and three independent angle-resolved Si2p and C1s spectra all give the same surface coverage very close to its theoretical limit.

1. Introduction

Since the early work of Chidsey and co-workers,^{1–4} hybrid interfaces coupling electronically an organic monolayer *directly* with a silicon substrate have received increasing interest because strong Si–C covalent bonding can easily be achieved via various chemical reactions.^{5,6} Direct proof of the covalent coupling between the silicon surface and the molecular moieties is generally difficult to obtain,^{2–4,7–9} and the robustness of monolayers is often taken as proof of the covalent molecular anchoring because the organic moieties seem to be irreversibly

immobilized on the silicon surface. The fact that monolayers prevent silicon etching is a further argument.^{10–12} In the context of applications of such hybrid interfaces, particularly for bio-electronics, comparing different derivatization routes becomes an issue to obtain the maximum possible coverage and prevent the degradation of interface properties in the long term. Keeping a very low density of interface states^{12–14} is particularly essential to improve device functioning. An optimization of the interface requires quantifying its composition (molecular density, linkage silicon–molecule, and chemistry at remaining ungrafted sites).

Structure-sensitive techniques such as X-ray diffraction or scanning probe microscopy are ineffective to determine a surface coverage in the case of organic monolayers on silicon surfaces because layers are generally disordered on the molecular scale.⁵ The system bromophenyl monolayers on Si(111) seems to be one exception with the observation of small 2 × 1 molecular

[†] Institut d'Electronique, de Microélectronique et de Nanotechnologie.

[‡] Laboratoire de Physique de la Matière Condensée.

- (1) Linford, M. R.; Chidsey, C. E. D. *J. Am. Chem. Soc.* **1993**, *115*, 12631.
- (2) Linford, M. R.; Fenter, P.; Eisenberger, P. M.; Chidsey, C. E. D. *J. Am. Chem. Soc.* **1995**, *117*, 3145.
- (3) (a) Terry, J.; Linford, M. R.; Wigren, C.; Cao, R.; Pianetta, P.; Chidsey, C. E. D. *Appl. Phys. Lett.* **1997**, *71*, 1056. (b) Terry, J.; Linford, M. R.; Wigren, C.; Cao, R.; Pianetta, P.; Chidsey, C. E. D. *J. Appl. Phys.* **1999**, *85*, 213.
- (4) Cicero, R. L.; Linford, M. R.; Chidsey, C. E. D. *Langmuir* **2000**, *16*, 5688.
- (5) For a review, see: Wayner, D. D. M.; Wolkow, R. A. *J. Chem. Soc., Perkin Trans.* **2002**, *2*, 23.
- (6) For a review, see: Buriak, J. *Chem. Rev.* **2002**, *102*, 1271.
- (7) Webb, L. J.; Lewis, N. S. *J. Phys. Chem. B* **2003**, *107*, 5404.
- (8) Zharnikov, M.; Kuller, A.; Shaporenko, A.; Schmidt, E.; Eck, W. *Langmuir* **2003**, *19*, 4682.
- (9) Fellah, S.; Teyssot, A.; Ozanam, F.; Chazalviel, J.-N.; Vigneron, J.; Etcheberry, A. *Langmuir* **2002**, *18*, 5851.

- (10) Yu, H.-Z.; Morin, S.; Wayner, D.; Allongue, P.; Henry de Villeneuve, C. *J. Phys. Chem. B* **2000**, *104*, 11157.
- (11) Allongue, P.; Henry de Villeneuve, C. *Electrochim. Acta* **2000**, *45*, 3241.
- (12) Allongue, P.; Henry de Villeneuve, C.; Cherouvrier, G.; Cortes, R. *J. Electroanal. Chem.* **2003**, *550–551*, 161.
- (13) Boukherroub, R.; Morin, S.; Sharpe, P.; Wayner, D. D. M.; Allongue, P. *Langmuir* **2000**, *16*, 7429.
- (14) Gorostiza, P.; Henry de Villeneuve, C.; Sanz, F.; Allongue, P. To be submitted for publication.

domains by STM.¹² X-ray reflectivity¹⁵ is a powerful technique to measure the true thickness of ultrathin films and the material density. Ellipsometry gives only qualitative indications and cannot be considered as really quantitative if performed at one single wavelength.^{1,2} Electrochemical capacitance measurements are rapid and give qualitative information about the surface coverage.^{10–12,14} X-ray photoelectron spectroscopy (XPS) is evidently a central surface technique combining both chemical and thickness sensitivity. Making XPS quantitative requires, however, dealing with two important questions. The first one concerns X-ray photodiffraction (XPD), a *built-in phenomenon* in XPS at ordered surfaces¹⁶ that has been used to investigate the atomic structure of solid-state interfaces and surfaces¹⁶ as well as the conformation of organic molecules at solid surfaces.^{17–19} Truly quantitative XPS measurements require accounting for XPD because it is responsible for azimuthal variations of the XPS signal intensity. This point has never been considered in recent XPS studies. The second issue concerns the photoelectron attenuation length (AL) in the organic film. AL can be calculated²⁰ but the result is not yet totally consistent with the existing experimental values.²¹ ALs have been measured for *n*-alkanethiol self-assembled monolayers (SAM) on Au(111) and some other substrates,^{22–24} and an in-depth XPS analysis was performed.²⁵

This work describes a simple experimental procedure to account for XPD in angle-resolved XPS measurements. It also describes three independent methods that aim at justifying that the AL of Si2p photoelectrons can be calculated using the empirical formula established by Laibinis and co-workers.²⁴ Thanks to these two precautions, we present a truly quantitative XPS study of alkyl and alkoxy monolayers directly grafted on atomically flat H–Si(111) surfaces. The complete compositional description of the interface is first achieved from the spectral decomposition of the Si2p and C1s core level spectra at a fixed polar angle. The results provide direct evidence that a Si–C and a Si–O–C linkage is formed, respectively, after reaction with decene and decanol and show that the interface is free of oxide. In a second approach, the different angle-resolved methods are used to determine the surface coverage. All methods give self-consistent results, and it is found that both kinds of monolayers are very dense with a molecular density quite close to its theoretical limit. A significant chain length dependence is also found.

2. Experimental Section

2.1. Sample Preparation. Silicon samples were cut from 10 Ω·cm *n*-type Si(111) wafers with 0.2° miscut angle along ⟨11–2⟩ purchased

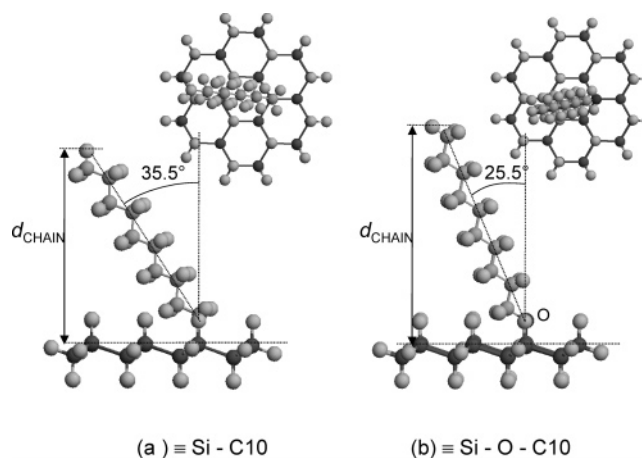
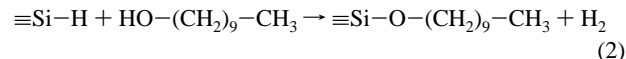
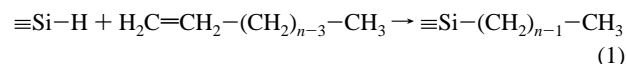


Figure 1. Optimized ball-and-stick molecular models of an Si–C10 (a) and Si–O–C10 (b) chain grafted on H–Si(111). A side view and a top view are shown in each case. d_{CHAIN} is the projection of the chain length on the surface normal (see eqs 3 and 4).

from Siltronix (France). Before organic modification, an atomically flat surface was prepared by controlled chemical etching in NH_4F as described elsewhere.^{26–29} Samples were first cleaned in hot H_2SO_4 (95%): H_2O_2 (30%) [2:1 in vol] mixture and copiously rinsed with 18.2 $\text{M}\Omega\cdot\text{cm}$ water. The H-termination was obtained by immersing the silicon in VLSI grade 40% NH_4F containing 50 mM $(\text{NH}_4)_2\text{SO}_3$ as oxygen scavenger.^{27,28}

The alkyl³⁰ and alkoxy¹³ monolayers on H–Si(111) surface were obtained by promoting the well-established reactions:



In both cases, the neat reagent was flushed with N_2 in a Schlenk tube heated at 100 °C to eliminate oxygen and water traces. After cooling to room temperature under continuous N_2 flushing, the freshly prepared H–Si(111) sample was introduced into the reactor. In the case of the reaction with alkenes, 10% of $\text{C}_2\text{H}_5\text{AlCl}_2$ was also added as catalyst (1 M solution in hexane, Aldrich). The two reactions were performed at 90 °C overnight (ca. 17 h) with the Schlenk tube carefully sealed to avoid contamination with oxygen or water traces. The sample was finally rinsed in tetrahydrofuran (THF) and 1,1,1-trichloroethane (TCE), and it was blown dried with N_2 . A first rinse with CF_3COOH (3% in THF) was necessary to neutralize residual $\text{C}_2\text{H}_5\text{AlCl}_2$ in the case of the reaction with alkenes. Samples modified by alkyl and alkoxy monolayers will be hereafter designated as $\equiv\text{Si}-\text{C}_n$ ($8 < n < 16$) or $\equiv\text{Si}-\text{O}-\text{C}_{10}$, where n is the number of carbon atoms.

In Figure 1 we show ball-and-stick molecular models of the two interfaces after optimization of the bond geometry (length and angles) using *Alchemy III* software (Tripos Inc., St Louis, MO). A slab consisting of a few silicon atoms assembled within a monolayer accounted for the silicon (111) surface. One single molecule was attached on top. The total energy was minimized around an initial configuration. The chain is shown stretched with no twist as expected for dense layers. In the case of the alkyl chain the measured chain tilt is 35.5° from the surface normal, which is consistent with other

(15) For a review, see: Tolan, M. *X-ray Scattering from Soft Matter Thin Films*; Springer: Berlin, 1999.

(16) For a detailed review on XPD, see: Westphal, C. *Surf. Sci. Rep.* **2003**, *50*, 1.

(17) Umbach, E. *Prog. Surf. Sci.* **1991**, *35*, 113.

(18) Bonzel, H. P. *Prog. Surf. Sci.* **1993**, *42*, 219.

(19) Barlow, S. M.; Raval, R. *Surf. Sci. Rep.* **2003**, *50*, 201.

(20) Jablonski, A.; Powell, C. J. *Surf. Sci. Rep.* **2002**, *47*, 33.

(21) Jablonski, A.; Salvat, F.; Powell, C. J. NIST Electron Elastic-Scattering Cross-Section Database, version 3.0; National Institute of Standards and Technology, 2002. <http://www.nist.gov/srd/nist64.htm>. (b) Lesiak, B.; Kosinski, A.; Krawczyk, M.; Zommer, L.; Jablonski, A.; Zemek, J.; Jiricek, P. P.; Kver, L.; Toth, J.; Varga, D.; Cserny, I. *Appl. Surf. Sci.* **1999**, *144–145*, 168.

(22) Bain, C. D.; Whitesides, G. M. *J. Phys. Chem.* **1989**, *93*, 1670.

(23) Lamont, C. L. A.; Wilkes, J. *Langmuir* **1999**, *15*, 2037.

(24) Laibinis, P. E.; Bain, C. D.; Whitesides, G. M. *J. Phys. Chem.* **1991**, *95*, 7017.

(25) Hansen, H. S.; Tougaard, S.; Biebuyck, H. J. *Electron Spectrosc. Relat. Phenom.* **1992**, *58*, 141.

(26) Wade, C. P.; Chidsey, C. E. D. *Appl. Phys. Lett.* **1997**, *71*, 1679.

(27) Fukidome, H.; Matsumura, M.; Komeda, T.; Mamba, K.; Nishika, Y. *Electrochim. Solid-State Lett.* **1999**, *2*, 393.

(28) Munford, M. L.; Corts, R.; Allongue, P. *Sens. Mater.* **2001**, *13*, 259.

(29) Allongue, P.; Henry de Villeneuve, C.; Morin, S.; Boukherroub, R.; Wayner, D. D. M. *Electrochim. Acta* **2000**, *45*, 4591.

(30) Boukherroub, R.; Bensebaa, F.; Morin, S.; Wayner, D. D. M. *Langmuir* **1999**, *15*, 3831.

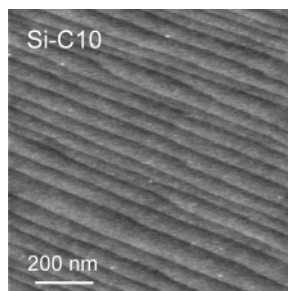


Figure 2. Typical contact mode AFM image ($1\ \mu\text{m} \times 1\ \mu\text{m}$) showing the staircase structure of the Si(111) surface after the organic modification with an alkyl monolayer. All modified surfaces look the same, and prolonged tip scanning does not remove adventitious material from the surface.

modeling.³¹ The neighboring surface sites are assumed to be occupied by H-atoms to be consistent with experiment (see section 4.1). Linford and Chidsey² hypothesized that the tilt angle is 45° to fit with the thickness derived from X-ray reflectivity. Neglecting the radius of the hydrogen atoms of the terminal methyl groups, the projected length d_{CHAIN} on the surface normal in Figure 1a may be expressed as:

$$d_{\text{CHAIN}} (\text{\AA}) = 1.89 + [n/2 - 1]2.54 \cos(35.5^\circ) + 1.56 \sin(19^\circ) + 1.1 \quad (3)$$

where n is *even*. The bond lengths and angles used in this expression were measured from Alchemy III. In the case of an alkoxy monolayer, the tilt angle is smaller (25.5°) because the measured Si–O–C bond angle is 118.3° (Figure 1b). This is again in close agreement with previous models.³² For such a layer the projected length reads (even n):

$$d_{\text{CHAIN}} (\text{\AA}) = 1.64 + [n/2 - 1]2.54 \cos(25.5^\circ) + 1.1 \sin(19^\circ) \quad (4)$$

2.2. Atomic Force Microscopy. The surface morphology was inspected by contact mode AFM (PicoSPM from Molecular Imaging, Phoenix, AZ) in a nitrogen atmosphere. Standard Si_3N_4 cantilevers with a spring constant $0.12\ \text{Nm}^{-1}$ (Nanoprobes) were employed. A successful surface modification leads to a staircase structure (Figure 2) identical to that of the H-terminated substrate, with atomically smooth terraces separated by monatomic steps ($3.14\ \text{\AA}$). There were, on average, only 10–20 protrusions per square micrometer of uniform height $0.3\ \text{nm}$ that were assigned to nanometer-oxide clusters, the surface coverage of which was below detection limit of XPS ($<1\%$). A uniform organic coverage may be inferred on the nanometer scale due to the absence of any contrast in friction images. Moreover, a prolonged tip scanning on the same place does not remove adventitious contamination or physisorbed molecules atop the monolayer. The modified surfaces are therefore clean on the molecular scale.

2.3. XPS Measurements. XPS measurements were performed using a Physical Electronics model 5600 spectrometer. A monochromatic Al $K\alpha$ X-ray source and an analyzer pass energy of $12\ \text{eV}$ were used. The acceptance angle was 14° . The resolution of the spectrometer is $0.55\ \text{eV}$ as measured from the full width at half maximum (fwhm) of the $\text{Ag}3d_{5/2}$ line. The intensity of XPS core levels was measured as the peak area after standard background subtraction according to the Shirley procedure.³³ The sample holder was modified to allow the rotations shown in Figure 3. The analyzed surface area A_{90} is a disk of diameter $0.4\ \text{mm}$ at $\theta = 90^\circ$. The takeoff angle θ is defined with a precision $\pm 1^\circ$. The typical sample size is $1 \times 1\ \text{cm}^2$. In the same set of experiments and using the same experimental conditions, the Si2p core level spectrum was recorded on a reference H-terminated Si(111) sample and the C1s core level spectrum was recorded on a highly

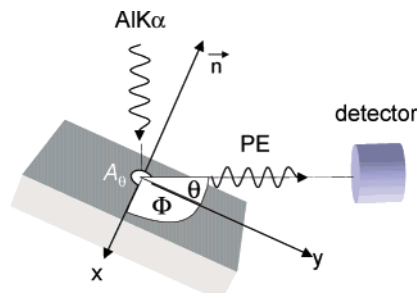


Figure 3. Definition of rotations used for XPS measurements: θ is the takeoff (or polar) angle, and the azimuth angle Φ corresponds to a rotation around the surface normal. $A_\theta = A_{90}/\sin \theta$ is the surface area analyzed at the takeoff angle θ .

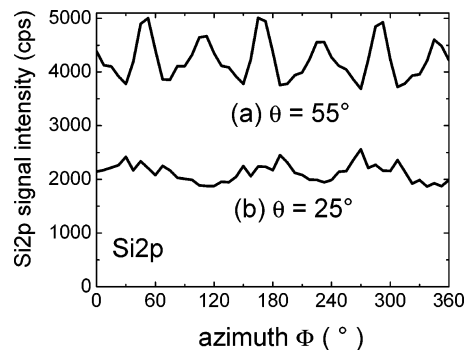


Figure 4. Integrated Si2p intensity as a function of the azimuth Φ for two different polar angles. The origin of Φ is arbitrary. The 120° periodicity arises from X-ray photodiffraction in specific crystallographic directions of the silicon substrate.

oriented pyrolytic graphite (HOPG) sample to serve as reference spectra in angle-resolved studies. The ratio of the Si2p and C1s core level intensity was then calculated to cancel intensity variations related to transmission changes with the detection angle.

The occurrence of XPD during XPS measurements may easily be put in evidence by plotting the signal intensity as a function of Φ . In Figure 4, the 120° periodic variations of the Si2p intensity measured on a H-terminated Si(111) surface arise from the threefold symmetry of the bulk silicon substrate. The intensity is remarkably enhanced by XPD in certain azimuths due to cooperative interferences in corresponding crystallographic directions. The phenomenon of XPD is indeed very similar to EXAFS:¹⁶ a spherical wave is directly emitted from an atom of the substrate, after the absorption of one X-ray photon, and is also elastically scattered at the near neighboring atoms.¹⁶ Both the direct and indirect waves interfere, and the resulting interference pattern is correlated to the interface atomic structure of the surface. One immediate consequence of Figure 4 is that successive *and* independent characterizations of the Si2p signal of the *very same* H-terminated sample would obligatorily lead to scattering of the Si2p signal intensity measurements due to the random value of Φ if the sample is placed without paying attention to its orientation on the support. Accordingly, the standard deviation of Si2p intensity would be as large as 30% for $\theta = 55^\circ$ or 25° . A similar effect is also anticipated after the organic modification with the supplementary complication that short-range atomic order in the organic layer may defocus the propagating wave. In other words, the periodic variations observed in Figure 4 might be altered in an unpredictable way at the modified surface.

As a consequence of XPD, attenuation measurements are dependent on the azimuth Φ , which does not allow anymore the use of eq 7 (section 3) to determine the attenuation length or the film thickness. To account for the influence of XPD at a given polar angle θ we have *averaged* the XPS signal by rotating the sample around its surface normal to make it exclusively sensitive to θ and independent of Φ . A motorized sample holder was installed in the spectrometer, and a large

(31) Sieval, A.; van der Hout, B.; Zuilhof, H.; Sudhölter, E. J. R. *Langmuir* **2001**, *17*, 2172.

(32) Pe, Y.; Ma, J.; Jiang, Y. *Langmuir* **2003**, *19*, 7652.

(33) Shirley, D. A. *Phys. Rev.* **1972**, *B5*, 4709.

acceptance angle of 14° was used.³⁴ All XPS spectra were acquired with this technique, which proved to be very efficient in the study of III–V semiconductor interfaces.³⁵

3. XPS Quantitative Analysis

This section describes different methods to analyze XPS data. The reader may consult reviews for more details.³⁶ The first method consists of measuring the attenuation of the Si2p signal after the organic modification. Within the continuum model, the Si2p signal intensity at the H-terminated and modified surface is given by:

$$S_{\text{si}}^{\text{H}} = KA_{90}\sigma_{\text{Si2p}}\rho_{\text{Si}}\lambda_{\text{Si}}(E_{\text{Si2p}}) \quad (5)$$

$$S_{\text{si}}^{\text{ML}} = KA_{90}\sigma_{\text{Si2p}}\rho_{\text{Si}}\lambda_{\text{Si}}(E_{\text{Si2p}}) \exp[-d/\lambda_{\text{ML}}(E_{\text{Si2p}}) \sin \theta] \quad (6)$$

where K is an instrumental constant; A_{90} is the (circular) surface area analyzed for a takeoff angle $\theta = 90^\circ$; σ_{Si2p} is the photoionization cross section for Si2p photoelectrons, ρ_{Si} is the atomic volume density in silicon, $\lambda_{\text{ML}}(E_{\text{Si2p}})$ and $\lambda_{\text{Si}}(E_{\text{Si2p}})$ are, respectively, the attenuation lengths of Si2p photoelectrons in the organic monolayer and in silicon, d is the monolayer thickness, and θ is the polar angle (Figure 3).

Dividing eq 6 by eq 5 yields the attenuation of the Si2p signal:

$$A_{\text{si}} = S_{\text{si}}^{\text{ML}}/S_{\text{si}}^{\text{H}} = \exp[-d/\lambda_{\text{ML}}(E_{\text{Si2p}}) \sin \theta] \quad (7)$$

A plot of $-\ln(A_{\text{si}})$ as a function of $1/(\sin \theta)$ can therefore be used to determine the film thickness. This approach is described in section 4.2. To compare the different methods, it is convenient to convert d into a surface coverage θ_{ML} using the relationship:

$$\theta_{\text{ML}} = (dD_{\text{Si}})/(d_{\text{CHAIN}}D_{\text{Au}}) \quad (8)$$

where d_{CHAIN} is the projected chain length (Figure 1) defined by the appropriate equation (3 or 4), $D_{\text{Si}} = 7.8 \times 10^{14} \text{ cm}^{-2}$ is the surface atom density on Si(111), and $D_{\text{Au}} = 4.63 \times 10^{14} \text{ cm}^{-2}$ is the surface density of alkanethiols in a perfect SAM on gold (Table 3).

The second angle-resolved method aims at determining the volume density of carbon atoms in the monolayer. This approach, encountered much less often in the literature, requires the use of a reference sample. We used an HOPG sample (see section 4.3). In analogy with the above equations, the C1s peak intensities arising from the organic film on silicon and from the HOPG substrate are given by:

$$S_{\text{C}}^{\text{ML}} = KA_{90}\sigma_{\text{C1s}}\rho_{\text{C,ML}}\lambda_{\text{ML}}(E_{\text{C1s}})\{1 - \exp[-d/\lambda_{\text{ML}}(E_{\text{C1s}}) \sin \theta]\} \quad (9)$$

$$S_{\text{C}}^{\text{HOPG}} = KA_{90}\sigma_{\text{C1s}}\rho_{\text{C,HOPG}}\lambda_{\text{HOPG}}(E_{\text{C1s}}) \quad (10)$$

where $\rho_{\text{C,ML}}$ and $\rho_{\text{C,HOPG}}$ are the carbon density in the monolayer and in HOPG, and $\lambda_{\text{ML}}(E_{\text{C1s}})$ and $\lambda_{\text{HOPG}}(E_{\text{C1s}})$ are the escape depths of C1s photoelectrons in the organic monolayer and in HOPG. All other symbols were defined above with the appropriate index. Dividing eq 9 by eq 10 yields:

$$R_{\text{C1s}} = S_{\text{C}}^{\text{ML}}/S_{\text{C}}^{\text{HOPG}} = B\{1 - \exp[-d/\lambda_{\text{ML}}(E_{\text{C1s}}) \sin \theta]\} \quad (11)$$

with

$$B = \rho_{\text{C,ML}}\lambda_{\text{ML}}(E_{\text{C1s}})/[\rho_{\text{C,HOPG}}\lambda_{\text{HOPG}}(E_{\text{C1s}})] \quad (12)$$

A plot of R_{C1s} as a function of $1/(\sin \theta)$ therefore gives access to $\rho_{\text{C,ML}}$ and d . It is easy to show that $\rho_{\text{C,ML}}$ may be converted into a surface coverage θ_{ML} using:

$$\theta_{\text{ML}} = \rho_{\text{C,ML}}d/n/D_{\text{Si}} \quad (13)$$

The last independent determination of the surface coverage consists of using the *relative* intensities of *specific* satellite peaks resolved in high-resolution core level spectra (section 4.1). For instance, the molecular coverage of an alkyl layer is equal to the surface density of C–Si bonds, which form one *atomic plane* of carbon atoms located at the interface (see Figure 1a). The C1s XPS signal intensity related to these carbon emitters is proportional to the total number of emitting centers times an exponential photoelectron attenuation factor to account for the presence of the organic layer. It reads:

$$S_{\text{C-Si}} = K\sigma_{\text{C1s}}(A_{90}N_{\text{C-Si}}/\sin \theta) \exp[-d^*/\lambda_{\text{ML}}(E_{\text{C1s}}) \sin \theta] \quad (14)$$

where $N_{\text{C-Si}}$ is the surface density of interfacial C–Si bonds, $A_{\theta} = A_{90}/\sin \theta$ accounts for the elliptic shape of the analyzed surface area at a polar angle θ (see Figure 3), and $d^* \approx d_{\text{CHAIN}} - 1.89 \text{ \AA}$ is the depth of the plane of carbon emitters measured from the top of the monolayer (see Figure 1). All other symbols have been defined above. Dividing eq 14 by eq 9 gives the *relative* intensity of the C–Si related peak in C1s spectra:

$$R_{\text{C-Si}} = G \exp[-d^*/\lambda_{\text{ML}}(E_{\text{C1s}}) \sin \theta] / \{1 - \exp[-d/\lambda_{\text{ML}}(E_{\text{C1s}}) \sin \theta]\} \quad (15)$$

with

$$G = N_{\text{C-Si}}/[\lambda_{\text{ML}}(E_{\text{C1s}})\rho_{\text{C,ML}}\sin \theta] = d/[n\lambda_{\text{ML}}(E_{\text{C1s}})\sin \theta] \quad (16)$$

The right-hand side term of eq 16 was obtained by combining eqs 13, 16 and 19 below. The thickness d was derived from $R_{\text{C-Si}}$ by solving numerically eq 15 and the surface coverage calculated using eq 8.

In the case of alkoxy monolayers, the relevant signal arises from silicon atoms involved in Si–O–C bonds provided the interface is oxide-free. Those Si emitting atoms again form one atomic plane of surface density $N_{\text{Si-O-C}}$ at a depth d measured from the top of the monolayer. In analogy with eq 14, the Si2p XPS signal intensity and relative intensity of the satellite peak are given by:

$$S_{\text{Si-O-C}} = D_{\text{Si}}\sigma_{\text{Si2p}}(A_{90}N_{\text{Si-O-C}}/\sin \theta) \exp[-d/\lambda_{\text{ML}}(E_{\text{Si2p}}) \sin \theta] \quad (17)$$

$$R_{\text{Si-O-C}} = N_{\text{Si-O-C}}/[\rho_{\text{Si}}\lambda_{\text{Si}}(E_{\text{Si2p}})\sin \theta] \quad (18)$$

The relationship between the surface densities $N_{\text{C-Si}}$ and $N_{\text{Si-O-C}}$ and the surface coverage θ_{M} is simply given by:

$$\theta_{\text{ML}} = N_{\text{C-Si}}/D_{\text{Si}} \quad \text{or} \quad N_{\text{Si-O-C}}/D_{\text{Si}} \quad (19)$$

(34) Seelmann-Eggebert, M.; Richter, H. *J. Phys. Rev.* **1991**, *B43*, 9578.

(35) Dehaese, O.; Wallart, X.; Schuler, O.; Mollot, F. *J. Appl. Phys.* **1998**, *84*, 2127.

(36) Fadley, C. S. *Prog. Surf. Sci.* **1984**, *16*, 275.

Table 1. List of Parameters Used for the Quantitative Analysis of XPS Spectra

	symbols	value
organic monolayer	$\lambda_{\text{ML}}(E_{\text{Si}2\text{p}})^a$	39.5 Å
	$\lambda_{\text{ML}}(E_{\text{O}1\text{s}})$	30 Å
	$\lambda_{\text{ML}}(E_{\text{C}1\text{s}})$	35.4 Å
silicon	$\lambda_{\text{Si}}(E_{\text{Si}2\text{p}})$	19 Å
	ρ_{Si}	5×10^{22} atoms/cm ³
HOPG	$\lambda_{\text{HOPG}}(E_{\text{C}1\text{s}})$	17 Å
	$\rho_{\text{C,HOPG}}$	1.13×10^{23} atoms/cm ³

^a Calculated from eq 20.

Exploiting the above equations requires the precise knowledge of photoelectron ALs at the relevant kinetic energies. For silicon, we used an average value of 19 Å between the 16 Å reported by Hochella et al.³⁷ and the 23 Å reported by Katayama et al.³⁸ For HOPG, the value of 17 Å was employed by averaging the λ -value of 13 Å derived from the formula of Seah and Dench³⁹ and the 21 Å derived from the formula given by Tanuma et al.^{20,40} The tabulated atomic densities ρ_{Si} and $\rho_{\text{C,HOPG}}$ are also given in Table 1. ALs in organic monolayers have been measured at *selected* kinetic energies (e.g., $E_{\text{Au}4f7/2}$) from angle-resolved measurements on SAMs of thiols on different single-crystal surfaces.²⁴ As will be justified later in the text, we will use the empirical formula

$$\lambda_{\text{ML}}(E_{\text{K}}) = 9 + 0.022E_{\text{K}} \quad (20)$$

to calculate the ALs necessary for this work, in particular $\lambda_{\text{ML}}(E_{\text{Si}2\text{p}})$. $\lambda_{\text{ML}}(E_{\text{K}})$ is expressed in angstroms, and the kinetic energy E_{K} is expressed in electronvolts. In the case of an Al K α source (1487 eV), the equation becomes $\lambda_{\text{ML}}(E) = 9 + 0.022(1487 - E)$, with E being the binding energy of the considered element. Thus calculated ALs $\lambda_{\text{ML}}(E_{\text{Si}2\text{p}})$, $\lambda_{\text{ML}}(E_{\text{O}1\text{s}})$, and $\lambda_{\text{ML}}(E_{\text{C}1\text{s}})$ are given in Table 1.

4. Results and Discussion

4.1. Composition of the Interface from Si2p and C1s Core Levels.

In survey XPS spectra (Figure S1, Supporting Information) the C1s peak is enhanced and the Si2p peak is attenuated after the organic modification. The oxygen content increases after reaction with decanol but remains quite low after the reaction with decene. In high-resolution Si2p spectra (Figure S2, Supporting Information), the attenuation of the doublet Si2p_{3/2} and Si2p_{1/2} (99.5 and 100.1 eV) is clear after the organic grafting. The important point concerns the absence of contribution related to oxide or suboxide species in the energy range 101–104 eV even though we used $\theta = 25^\circ$ to maximize surface sensitivity. Subtle differences in interface composition are better evidenced by *normalized* Si2p spectra. Figure 5a shows that all spectra quasi perfectly overlap with one another except that of the alkoxy monolayer, for which a supplementary doublet (chemical shift $\Delta E = -0.7$ eV and relative intensity 11%) is necessary to fit the entire spectrum (Figure 5b). The C1s core level spectra present more obvious differences apart from the main component at 285.2 eV assigned to the aliphatic chains (Figure 6). In the case of the $\equiv\text{Si}-\text{O}-\text{C}10$ layer (Figure 6a), one satellite component is found at higher binding energy (286.1

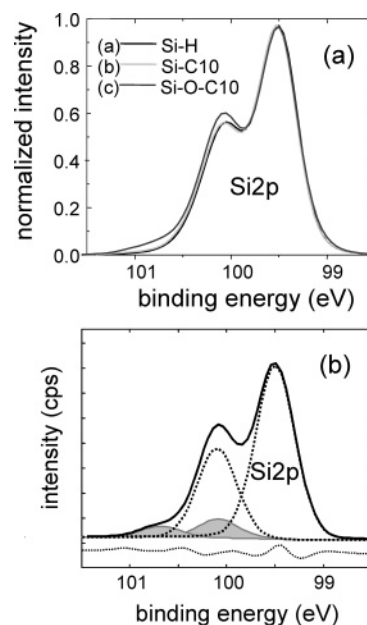


Figure 5. (a) Normalized Si2p spectra recorded at a polar angle $\theta = 25^\circ$ (raw spectra are given in Supporting Information, Figure S2). Notice that the spectra of the H–Si(111) and the $\equiv\text{Si}-\text{C}10$ samples are quasi-identical while the one of the $\equiv\text{Si}-\text{O}-\text{C}10$ sample is slightly different at higher binding energies. (b) Spectral decomposition of the spectrum of the $\equiv\text{Si}-\text{O}-\text{C}10$ layer. The fit residual (dotted line) was shifted downward for clarity.

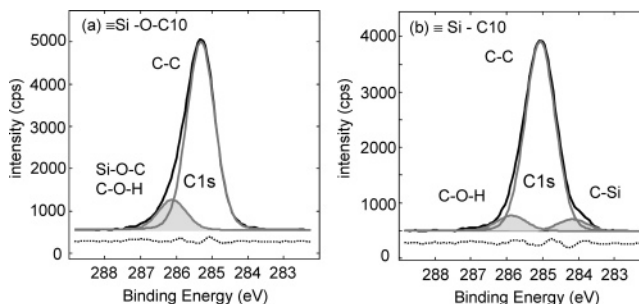


Figure 6. High-resolution C1s core level spectra of a $\equiv\text{Si}-\text{O}-\text{C}10$ (a) and a $\equiv\text{Si}-\text{C}10$ (b) sample recorded at a polar angle $\theta = 25^\circ$. The black line is the measured signal. The gray lines correspond to the spectral decomposition. The fit residual (dotted line) was shifted downward for clarity.

Table 2. Quantitative Analysis of the Satellite Peaks in Si2p and C1s Core Level XPS Spectra of Figures 5 and 6^a

surface	Si2p		C1s
chemical shift	$E = 0.7$ eV	$E = 0.7-0.9$ eV	$E = -0.9$ eV
bond assignment	(Si–O–C)	(C–OH, C–O–Si)	(C–Si)
H–Si(111)	– ^b	–	–
$\equiv\text{Si}-\text{C}10$	–	0.08/– ^c	0.07/0.48
$\equiv\text{Si}-\text{O}-\text{C}10$	0.11/0.52 ^d	0.16/0.48 ^e	–

^a The chemical shift and the possible bond assignment are indicated for each peak. The measured *relative* intensity of satellite components and the calculated surface coverage using the relevant equations given in section 3 are given in the bottom lines. ^b (–) = intensity not measurable or below detection limit. ^c Coverage not calculated because the satellite peak is partly related to contamination (see text). ^d Estimate assuming that the intensity is uniquely related to Si atoms involved in Si–O–C bonds. ^e Estimate after correction of the signal arising from adventitious contaminations (see text).

eV, $\Delta E = 0.9$ eV). Two satellite peaks at 285.9 eV ($\Delta E = 0.7$ eV) and 284.2 eV ($\Delta E = -0.9$ eV) are resolved with the $\equiv\text{Si}-\text{C}10$ layer (Figure 6b); Table 2 lists the characteristics of the above satellite peaks.

(37) Hochella, M. F., Jr.; Carim, A. H. *Surf. Sci.* **1988**, *197*, L260.

(38) Katayama, T.; Yamamoto, H.; Ikeno, M.; Mashiko, Y.; Kawazu, S.; Umeno, M. *Jpn. J. Appl. Phys.* **1999**, *38*, L770.

(39) Seah, M. P.; Dench, W. A. *Surf. Interface Anal.* **1979**, *1*, 2.

(40) Tanuma, S.; Powell, C. J.; Penn, D. R. *Surf. Interface Anal.* **1988**, *11*, 577.

Binding and Coverage at the $\equiv\text{Si}-\text{C}10$ Interface. After reaction with 1-decene, the formation of interfacial Si–C bonds must be anticipated from reaction 1. It is nevertheless practically impossible to assess their existence because the Si2p peak is quasi-identical to that of the H-terminated (Figure 5a). The relevant information is obtained from the C1s spectrum, in which the satellite peak with chemical shift $\Delta E = -0.9$ eV may be assigned to C–Si bonds if one considers the difference in Pauling's electronegativity of silicon (1.9) and carbon (2.55). Assigning this satellite peak to C–Si bonds is also justified by its absence in the C1s spectrum of the alkoxy layer (Figure 6a). Liu and Hamers made the same assignment in the case of Si(001) surfaces after molecular adsorption in the UHV.⁴¹ The C–Si related peak was more prominent in their spectra because shorter molecules were used. In our case, the relative intensity of the C–Si related contribution (7%) is close to expectations for a chain with 10 carbon atoms. A more precise analysis requires the use of eqs 15, 16, and 19. Numerically, $R_{\text{C-Si}} = 0.07$ leads to $d = 9.6 \pm 0.2$ Å or a surface coverage of $\theta_{\text{ML}} = 0.48 \pm 0.01$ (Table 2). This value is very close to the theoretical limit of 0.5.³¹ We used $n = 10$, $\theta = 25^\circ$, and $\lambda_{\text{ML}}(E_{\text{C1s}}) = 35.4$ Å (Table 1) in calculation. The value of $\lambda_{\text{ML}}(E_{\text{C1s}})$ will be justified a posteriori in sections 4.2 and 4.3. The only XPS signal in Figure 6b, which cannot be attributed to the very interface, is the small contribution at 286.1 eV in the C1s spectrum (8% of the main peak), which is assigned to adventitious contamination representing less than 0.05 ML.

Binding and Coverage at the $\equiv\text{Si}-\text{O}-\text{C}10$ Interface. The Si2p satellite peak with a positive chemical shift 0.7 eV (Figure 5b) may be assigned to a Si–O–C linkage, as expected from reaction 2, but also to eventual silanol groups or suboxide species. In all cases, the silicon atom is indeed positively charged due to the electronegativity difference of Si and O. If one tentatively attributes the relative signal $R_{\text{Si-O-C}} = 0.11$ to the sole Si emitting atoms involved in Si–O–C bonds, one finds the surface density $N_{\text{Si-O-C}} = 4.03 \cdot 10^{14}$ cm⁻² (eq 18) and the surface coverage is 0.52 (eq 19). Unfortunately, a cross verification cannot be obtained from the signal $R_{\text{O-C}}$ arising from carbon atoms involved in C–O bonds using an equation similar to eq 15. The calculated surface coverage is indeed ~ 0.97 , which is too large³² and signifies the presence of adventitious surface contaminations. We used $d^* \approx d_{\text{CHAIN}} - 1.69$ Å (see Figure 1 and eq 4). If one tentatively assumes the same level of contamination as that on the alkyl monolayer, the surface coverage would be 0.48 ($R_{\text{O-C}} = 0.16-0.08$; see Table 3), which is close to 0.52. An independent cross verification of these estimates is obtained from the plot $A_{\text{Si}}(1/\sin \theta)$ (result not shown). As in Figure 7, such a method allows measuring d from the slope $d/\lambda_{\text{ML}}(E_{\text{Si2p}}) = 0.251$. One finds $d = 9.9$ Å and $\theta_{\text{ML}} = 0.42$.

In conclusion of this section, the formation of Si–C and Si–O–C bonds, respectively, after reaction with decene and decanol, is unambiguously attested from the spectral decomposition of Si2p and C1s core levels. In the case of the $\equiv\text{Si}-\text{C}10$

Table 3. Characteristics of Si(111), Au(111) Surfaces, and Maximum Molecular Density of Aliphatic Chains on the Same Surfaces and in Crystallized Polyethylene (PE)^a

	Si(111)	Au(111)	PE ^d
surface density (atoms/cm ²)	$D_{\text{Si}} = 7.8 \times 10^{14}$	$D_{\text{Au}} = 1.39 \times 10^{15}$	18.4
unit cell (Å ²)	12.8	7.2	–
maximum coverage in ML	0.5	0.33	5.4×10^{14}
maximum density (molecules/cm ²)	3.9×10^{14b}	4.63×10^{14c}	1.17
relative maximum molecular density	0.84	1	

^a Data for SAMs on Au(111) and PE were taken from refs 42–44. ^b Corresponding to an ideal 2×1 structure. ^c Corresponding to a $(\sqrt{3} \times \sqrt{3})R30^\circ$ structure. ^d Polyethylene has an orthorhombic crystallographic structure of unit cell ($a = 4.96$ and $b = 7.42$). The chains are parallel to the c -axis.

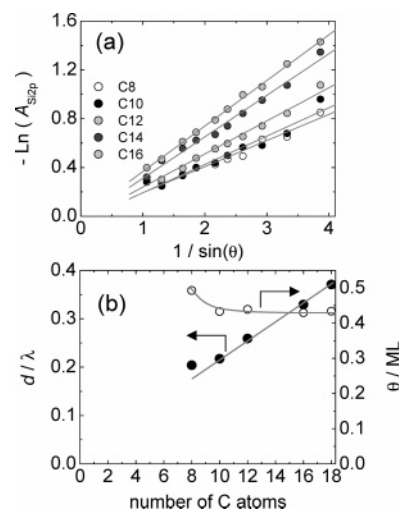


Figure 7. Angle-resolved measurements of the Si2p attenuation: (a) Plots of $-\text{Ln}(A_{\text{Si}})$ as a function of $1/\sin \theta$. The chain length is expressed in the number of carbon atoms per chain (see figure). Solid lines are best linear fits. (b) Filled symbols: variations of $d/\lambda_{\text{ML}}(E_{\text{Si}})$ derived from the slopes measured in (a). Open symbols: variations of the layer coverage θ_{ML} calculated using eq 8.

layer, the surface coverage is 0.48 (Table 2) and Si–H bonds saturate ungrafted sites. In the case of the $\equiv\text{Si}-\text{O}-\text{C}10$ layer, the estimate of the coverage is more subject to hypothesis about contaminations and a possible limited oxidation. From cross correlations we find that the surface coverage is in the range 0.42–0.52. Most of the ungrafted sites are probably saturated with Si–H bonds because a low density of interface state is found from capacitance measurements.¹⁴

4.2. Monolayer Surface Coverage from Si2p Angle-Resolved Measurements. From eq 7 a plot of $-\text{Ln}(A_{\text{Si}})$ as a function of $(1/\sin \theta)$ should be a straight line with slope $d/\lambda_{\text{ML}}(E_{\text{Si2p}})$ yielding d if $\lambda_{\text{ML}}(E_{\text{Si2p}})$ is known. The series of straight lines displayed in Figure 7a is in perfect agreement with this expectation: $d/\lambda_{\text{ML}}(E_{\text{Si2p}})$ is indeed proportional to the chain length (Figure 7b) and all best linear fits extrapolate through the origin, which is a strong indication that monolayers are homogeneous and do not present extended defects. Note that the slope (0.0189 ± 0.0008) in Figure 7b would correspond to an AL of Si2p photoelectrons $\lambda_{\text{ML}}(E_{\text{Si2p}}) = 54.5 \pm 2$ Å by assuming that the monolayer thickness $d = d_{\text{CHAIN}}$ (see Figure 1). This approach cannot be used because this assumption overestimates d , and d is indeed smaller than d_{CHAIN} because

- (41) (a) Liu, H.; Hamers, R. J. *Surf. Sci.* **1998**, *416*, 354. (b) Liu, Z. H.; McCaffrey, J. P.; Brar, B.; Wilk, G. D.; Wallace, R. M.; Feldman, L. C.; Tay, S. P. *Appl. Phys. Lett.* **1997**, *71*, 2764.
 (42) (a) Whitesides, G. M.; Laibinis, P. E. *Langmuir* **1990**, *6*, 87. (b) Ulmann, A. *Ultrathin Organic Films*; Academic Press: San Diego, CA, 1991. (c) Ulmann, A. *Adv. Mater.* **1990**, *2*, 573.
 (43) Poirier, G. E. *Chem. Rev.* **1997**, *97*, 117.
 (44) Dorset, D. L. *J. Phys. Chem. B* **2000**, *104*, 8346.

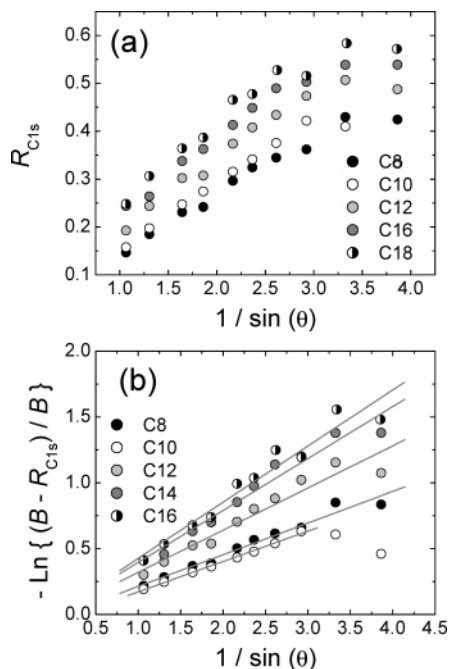


Figure 8. Angle-resolved C1s measurements on alkyl monolayers on Si(111) and HOPG. (A) Plots of R_{C1s} as a function of $1/\sin(\theta)$ (see eq 11). (B) Plots of $-\ln\{(B - R_{C1s})/B\}$ as a function of $1/\sin(\theta)$. For each chain length, B was adjusted to obtain a straight line passing through the origin (see eq 11). The chain length is indicated in the figures.

an ideally 2×1 structure on Si(111) is 16% less dense than a $(\sqrt{3} \times \sqrt{3})R30^\circ$ n -alkanethiol SAM on Au(111) and 39% less dense than in polyethylene (Table 3).

Our original idea was to consider the AL of the most compact system, but no AL value is available for Si2p photoelectrons in polyethylene (Table 3). We tentatively assumed that SAMs of alkanethiols are perfect “single-crystal organic monolayers” (SAMs are close-packed on the molecular scale and present large molecular ordered domains) and calculated the Si2p photoelectron AL using eq 20. Namely, we injected $\lambda_{ML}(E_{Si2p}) = 39.5 \text{ \AA}$ (Table 1) into eq 7 to determine d and then θ_M (eq 8). Within this analysis, we find that $0.43 < \theta_M < 0.49$ (Figure 7b, open symbols), with a significant increase of θ_M as the molecule shortens. This trend is a manifestation of surface shielding during molecular grafting. As soon as a molecular chain is (irreversibly) anchored on the surface, some of the six next-neighboring surface sites become practically inaccessible to molecules arriving from the solution side although the same sites would be sterically allowed in a real self-assembling process. The longer the molecular chain, the greater the shielding of the surface (Figure 1). Finally, we note the close agreement between $\theta_{ML} = 0.44$ for $n = 10$ in Figure 7 and the surface coverage found in section 4.1 (0.48, see Table 2). This constitutes a first justification of our approach. Additional arguments will be provided later on.

4.3. Monolayer Surface Coverage from C1s Angle-Resolved Measurements. Equations 11 and 12 show that the angle-resolved study of the C1s signal on the modified silicon surface and on HOPG allows determination of the volume density of carbon atoms in the monolayers. Plots of R_{C1s} versus $1/\sin(\theta)$ are displayed in Figure 8a for different molecular chain lengths. They were fitted with a two-step procedure to derive $d/\lambda_{ML}(E_{C1s})$ and B . We first determined B by plotting $-\ln\{(B - R_{C1s})/B\}$

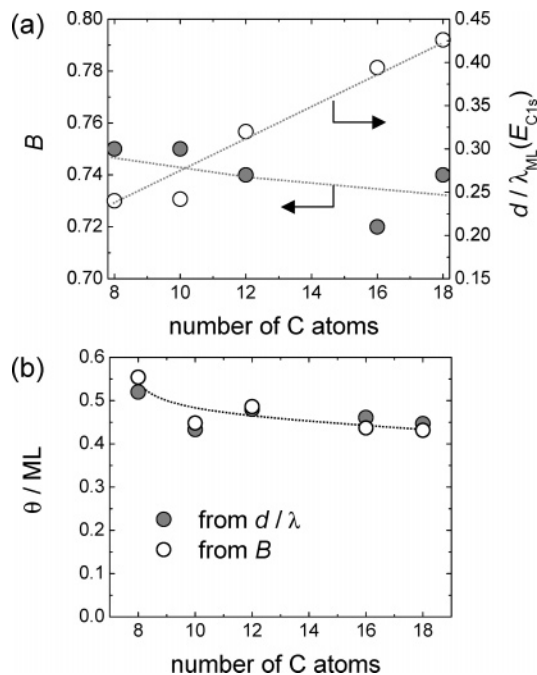


Figure 9. Angle-resolved C1s measurements on alkyl monolayers on Si(111) and HOPG. (A) Variations of $d/\lambda_{ML}(E_{C1s})$ and B (eq 12) as a function of the chain length. (B) Corresponding variations of θ_{ML} derived from $d/\lambda_{ML}(E_{C1s})$ (filled symbols) and B (open symbols).

$-\ln\{(B - R_{C1s})/B\}$ versus $1/\sin(\theta)$ (Figure 8b) with B as an adjustable parameter so as to minimize the ordinate at origin of the obtained straight lines and to be consistent with eq 11. The value of $d/\lambda_{ML}(E_{C1s})$ was subsequently measured from the slopes in Figure 8b. The chain length dependence of B (filled symbols) and $d/\lambda_{ML}(E_{C1s})$ (open symbols) are given in Figure 9a.

The knowledge of B gives directly the volume density $\rho_{C,ML}$ with no assumption since all parameters but $\rho_{C,ML}$ are known in eq 12. The corresponding chain length dependence of θ_{ML} (eq 13) is shown in Figure 9b (open symbols). The measure of $d/\lambda_{ML}(E_{C1s})$ from Figure 8b yields also θ_{ML} using $\lambda_{ML}(E_{C1s}) = 35.4 \text{ \AA}$ in calculation (Figure 9b, filled symbols). The two determinations of θ_{ML} agree very well. They can be considered independent because the use of B does not involve any assumption on $\lambda_{ML}(E_{C1s})$. This excellent agreement pertains, therefore, to the use of eq 20 to calculate $\lambda_{ML}(E_{C1s}) = 35.4 \text{ \AA}$. Additionally, these last determinations are also in close agreement with those in Figure 7b (open symbols). Hence, all three angle-resolved methods give coherent results and corroborate a chain length dependence of θ_{ML} .

5. Conclusions

We have demonstrated that accounting for X-ray photodiffraction is necessary for a truly quantitative XPS analysis of organic monolayers on ordered surfaces. By averaging the Si2p XPS signal over the azimuth angle, the Si2p XPS signal intensity becomes independent of the sample orientation on the sample holder. The second key point concerned the Si2p and C1s photoelectron attenuation lengths. From three independent angle-resolved methods we have established that the corresponding ALs can be calculated using eq 20.²⁴ For the case of alkyl and alkoxy monolayers on atomically flat Si(111) surfaces, we have shown that very dense monolayers can be prepared, with a surface coverage very close to its maximum theoretical limit.

In addition, it was unambiguously established that a Si–C and Si–O–C linkage is formed after reaction with alkenes and decanol, respectively, and that the ungrafted sites remain H-terminated.

Acknowledgment. This work was partially financed by the *Programme Matériaux* of CNRS and Ministère de la Recherche et de la Technologie.

Supporting Information Available: XPS survey spectra of as-prepared Si(111) surfaces and high-resolution Si2p core level spectra of as-prepared different Si(111) surfaces. This material is available free of charge via the Internet at <http://pubs.acs.org>.

JA0430797